

# Selective Adsorption and Photocatalytic Degradation of Extracellular Antibiotic Resistance Genes by Molecularly-Imprinted Graphitic Carbon Nitride

Qingbin Yuan,<sup>†, #</sup> Danning Zhang,<sup>‡, §, #</sup> Pingfeng Yu,<sup>\*, ‡, §</sup> Ruonan Sun,<sup>‡, §</sup> Hassan Javed,<sup>‡, §</sup>

Gang Wu,<sup>||</sup> and Pedro J.J. Alvarez<sup>\*, ‡, §</sup>

<sup>†</sup> College of Environment Science and Engineering, Nanjing Tech University, Nanjing, Jiangsu 211816, China

<sup>‡</sup> Department of Civil and Environmental Engineering, Rice University, Houston, Texas 77005, United States

<sup>§</sup> Nanosystems Engineering Research Center for Nanotechnology Enabled Water Treatment (NEWT), Houston, Texas 77005, United States

<sup>||</sup> Department of Internal Medicine, University of Texas–McGovern Medical School, Houston, Texas 77030, United States

<sup>#</sup> Q. Yuan and D. Zhang contributed equally.

\*Email: [pingfeng.yu@rice.edu](mailto:pingfeng.yu@rice.edu) (P.Y.)

\*Email: [alvarez@rice.edu](mailto:alvarez@rice.edu) (P.J.J.A.)

The supporting information includes:

Methods

1. Synthesis of carboxylic carbon nitride (CN-COOH).
2. ARG quantification via quantitative PCR (qPCR).

Figures

Figure S1. Circular map of plasmid pET-29a(+):*bla*<sub>NDM-1</sub>.

Figure S2. The morphology and thickness of g-C<sub>3</sub>N<sub>4</sub> and MIP-C<sub>3</sub>N<sub>4</sub> under AFM.

Figure S3. XRD pattern of carbon nitride (C<sub>3</sub>N<sub>4</sub>) and carboxylic carbon nitride (C<sub>3</sub>N<sub>4</sub>-COOH).

Figure S4. Raman spectrum of C<sub>3</sub>N<sub>4</sub>, MIP-C<sub>3</sub>N<sub>4</sub> and NIP-C<sub>3</sub>N<sub>4</sub>.

Figure S5. The UV-VIS DRS spectra of bare C<sub>3</sub>N<sub>4</sub>, MIP-C<sub>3</sub>N<sub>4</sub> and NIP-C<sub>3</sub>N<sub>4</sub>.

Figure S6. FTIR spectra of guanine imprinted MIP-C<sub>3</sub>N<sub>4</sub> with different MIP contents (18.6%, 24.7%)

and 30.2%) and after 10 reuse cycles.

Figure S7. XPS spectra of carbon nitride with vinyl groups ( $C_3N_4-C=CH_2$ ).

Figure S8. Lack of ARG removal in DI water by MIP- $C_3N_4$  without UVA irradiation or by photolysis with UVA irradiation alone.

Figure S9. Adsorption isotherm and kinetics of  $bla_{NDM-1}$  by MIP- $C_3N_4$  or NIP- $C_3N_4$  in DI water.

Figure S10. Photocatalytic degradation and adsorption removal of oligonucleotides with different guanine contents by MIP- $C_3N_4$ ,  $C_3N_4$ , and P25 in DI water.

Figure S11. ESR spectra of MIP- $C_3N_4$  and NIP- $C_3N_4$  before and after spiked with  $\bullet OH$  scavenger (IPA).

Figure S12. The UV-Vis spectrum of  $bla_{NDM-1}$  sample treated by MIP- $C_3N_4$  photocatalytic reaction at different times.

Figure S13. The melting curve of  $bla_{NDM-1}$  sample treated by adsorption and photocatalytic reaction.

Figure S14. Reusability of MIP- $C_3N_4$  and P25  $TiO_2$  in secondary effluent. Catalysts were tested for 10 cycles.

Figure S15. SEM images of MIP- $C_3N_4$  after 10 cycles of reuse in secondary effluent.

## Tables

Table S1. Water quality data of the secondary effluent from a wastewater treatment plant in Houston.

Table S2. Specific surface area of different catalysts.

Table S3. Chemical bonds composition of MIP- $C_3N_4$  pretreated with different oxidation time and their photoactivity.

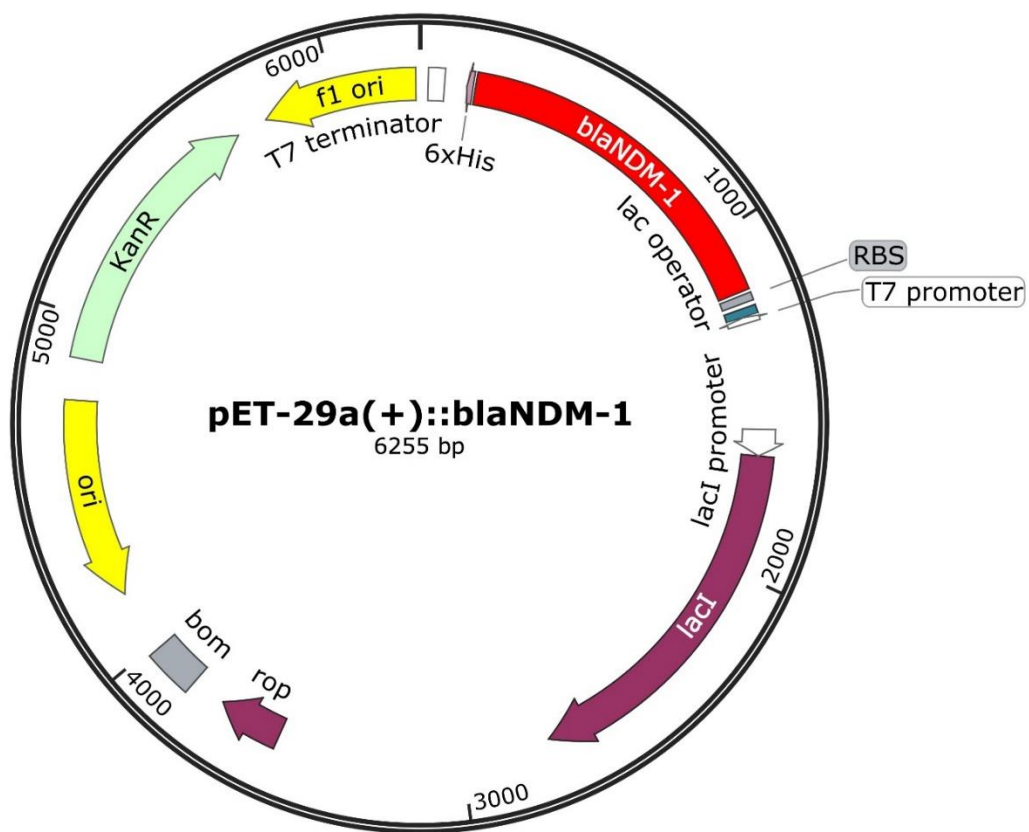
Table S4. First-order rate constant (k) of  $bla_{NDM-1}$  removal by MIP- $C_3N_4$  or NIP- $C_3N_4$ ,  $C_3N_4$  and  $TiO_2$  in different water matrix.

Table S5. Total read count and average DNA length of  $bla_{NDM-1}$  sample after treated by MIP- $C_3N_4$  or NIP- $C_3N_4$ .

## References

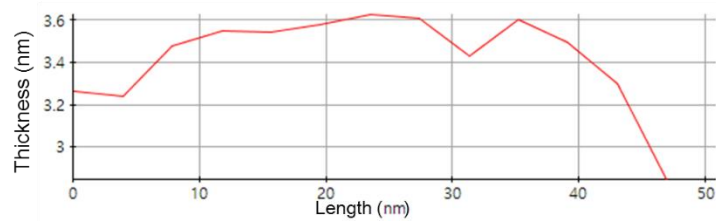
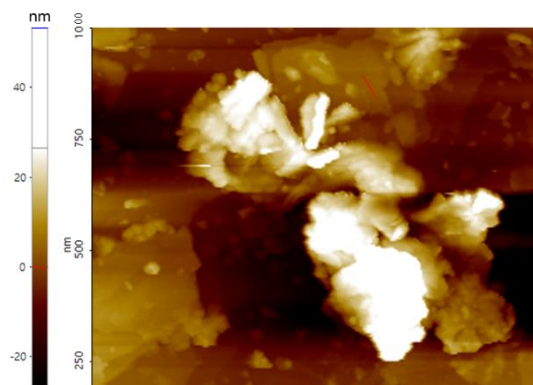
**Synthesis of carboxylic carbon nitride (CN-COOH).** Carboxylic carbon nitride (CN-COOH) was synthesized as previous reported.<sup>1</sup> Briefly, 1.0 g of g-C<sub>3</sub>N<sub>4</sub> was dissolved in 30 mL concentrated sulfuric acid (> 98%) and heated at 80 °C for 60 min under vigorous stirring. The solution was then cooled in ice-bath and 1.2 g of KMnO<sub>4</sub> was slowly added after the temperature of the solution reaches 0 °C (caution: KMnO<sub>4</sub> must not be added abruptly, otherwise intensive temperature increase may cause explosion). The solution was then heated at 30 °C for oxidation. By manipulating the oxidation time, CN-COOH with various content of carboxylic group can be achieved. After oxidation in the previous step, 200 mL deionized water was moderately dropped into the above solution. The temperature of the solution should be strictly controlled between 30 to 35 °C. Then, 50 mL of hydrogen peroxide aqueous solution (5% v/v) was added and the color of the solution changed from dark brown to white. The precipitates were collected, washed with 5 % HCl and water sequentially to remove any excessive impurities. CN-COOH was obtained after drying the washed precipitates in vacuum drying oven under 40 °C overnight.

**ARG quantification via quantitative PCR (qPCR).** The standard curve (*C<sub>t</sub>* value versus log of ARG copies) was generated using 10-fold serial dilution of the plasmids. The reaction mixture with a final volume of 15 µL contain 7.5 µL of SYBR Green Master Mix (Thermo Fisher Scientific, U.S.), 0.5 µL of each primer (10 µM) and 1 µL of the template DNA. Thermal cycling and fluorescence detection were conducted on a CFX 96 Real-time Systems (BIO-RAD, U.S.) using the following protocol: 50 °C for 2 min, 95 °C for 2 min, followed by 40 cycles of 95 °C for 15 s, 57 °C for 30 s and 72 °C for 30 s. Each reaction was run in triplicate. The specificity of the qPCR products was further verified by melting curves.



**Figure S1.** Circular map of plasmid pET-29a(+)::bla<sub>NDM-1</sub>. The length of bla<sub>NDM-1</sub> (red fragment) is 813bp and that of the whole plasmid is 6255 bp.

(a)  $C_3N_4$



(b) MIP- $C_3N_4$

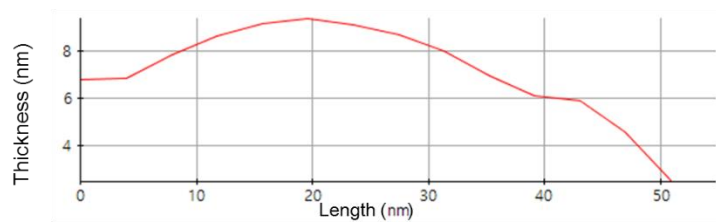
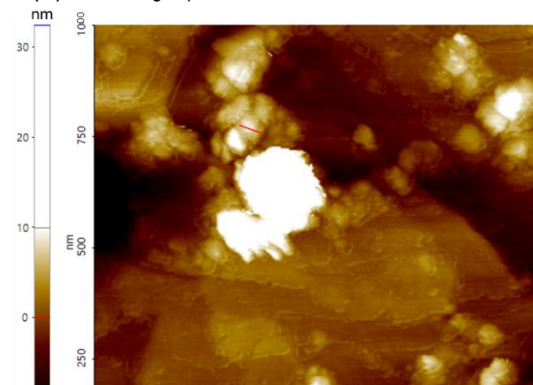


**Figure S2.** The morphology and thickness of  $C_3N_4$  and MIP- $C_3N_4$  under AFM.

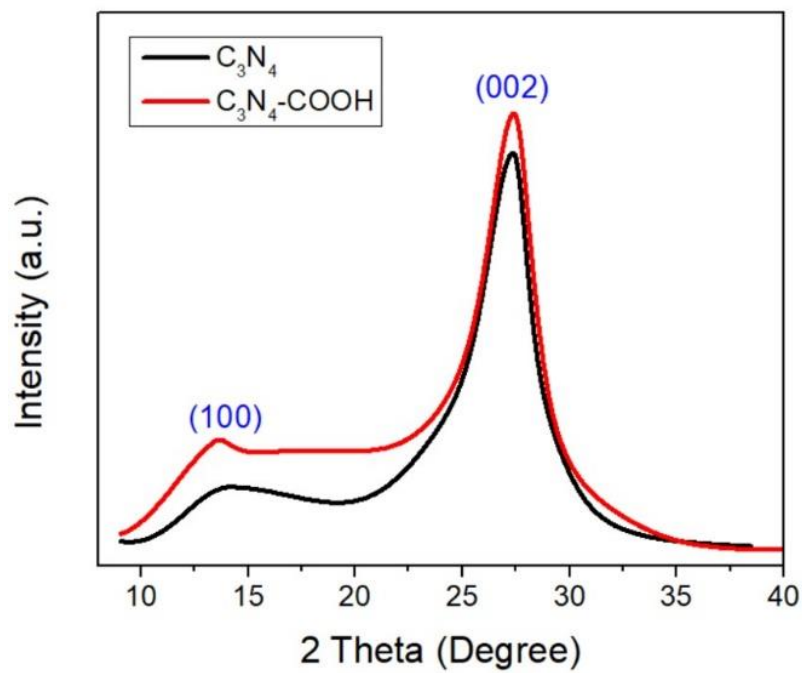


**Figure S3.** XRD pattern of graphite-like carbon nitride ( $C_3N_4$ ) and carboxylic carbon nitride ( $C_3N_4$ -COOH) with Cu K $\alpha$  radiation ( $\lambda = 1.54178 \text{ \AA}$ ).

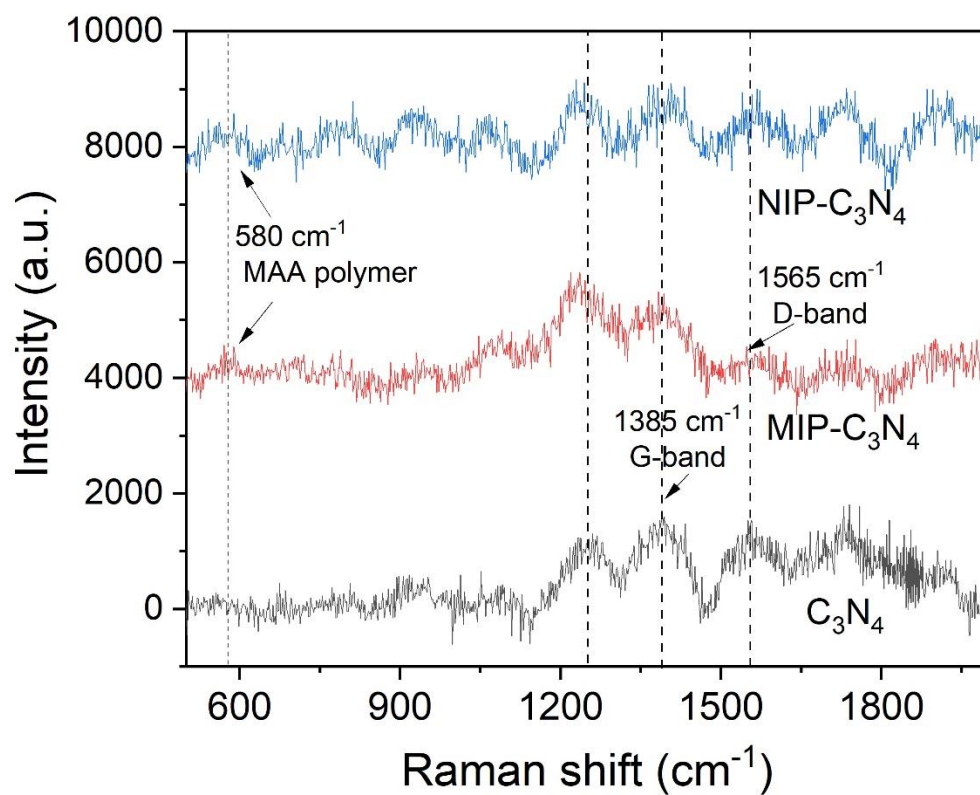


**Figure S4.** Raman spectrum of C<sub>3</sub>N<sub>4</sub>, MIP-C<sub>3</sub>N<sub>4</sub> and NIP-C<sub>3</sub>N<sub>4</sub>.

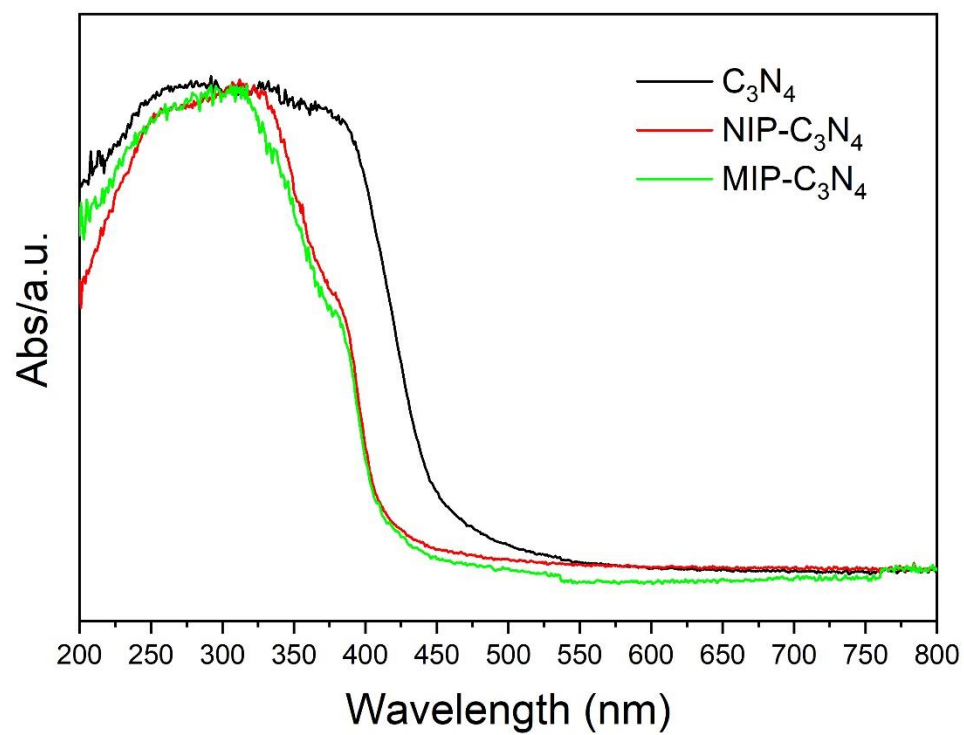


**Figure S5.** The UV-VIS DRS spectra of bare  $C_3N_4$ , MIP- $C_3N_4$  and NIP- $C_3N_4$ .



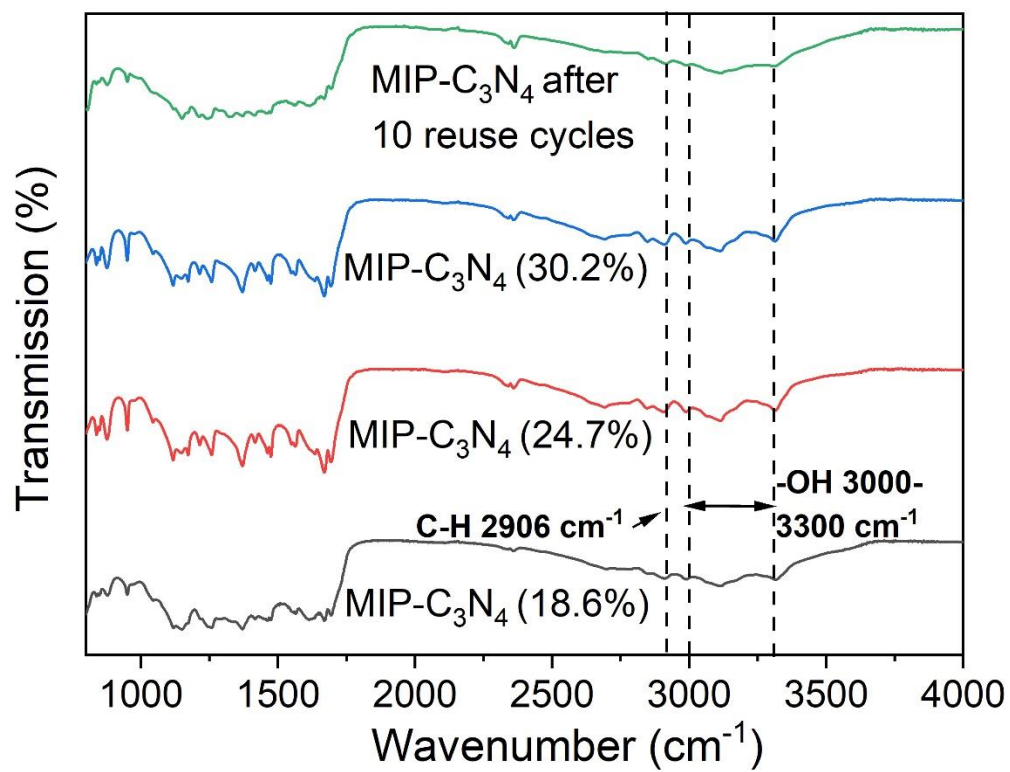


**Figure S6.** FTIR spectra of guanine imprinted MIP- $\text{C}_3\text{N}_4$  with different MIP contents (18.6%, 24.7% and 30.2%) and after 10 reuse cycles.

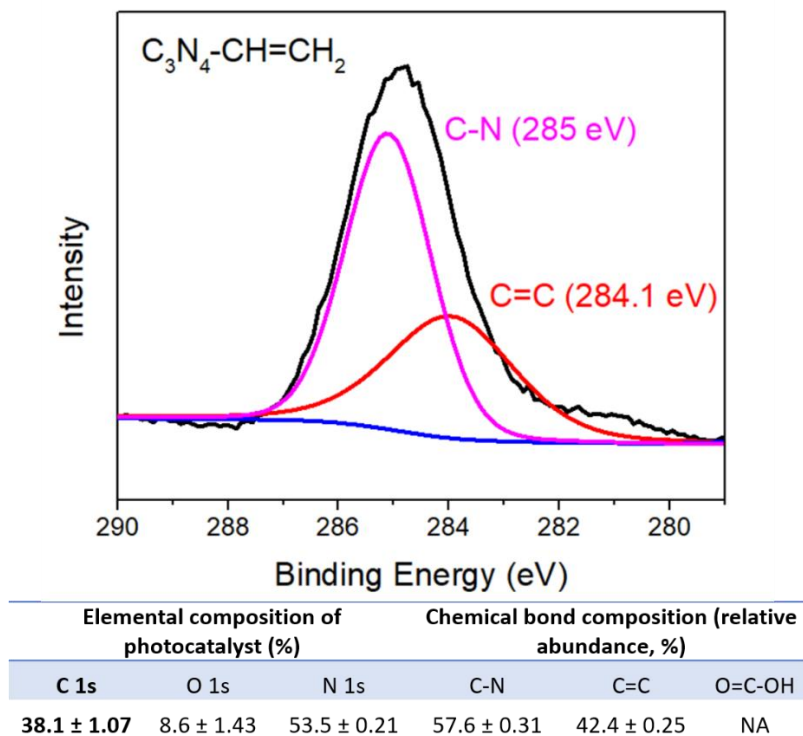


**Figure S7.** XPS spectra of carbon nitride with vinyl groups ( $\text{C}_3\text{N}_4\text{-CH=CH}_2$ ).

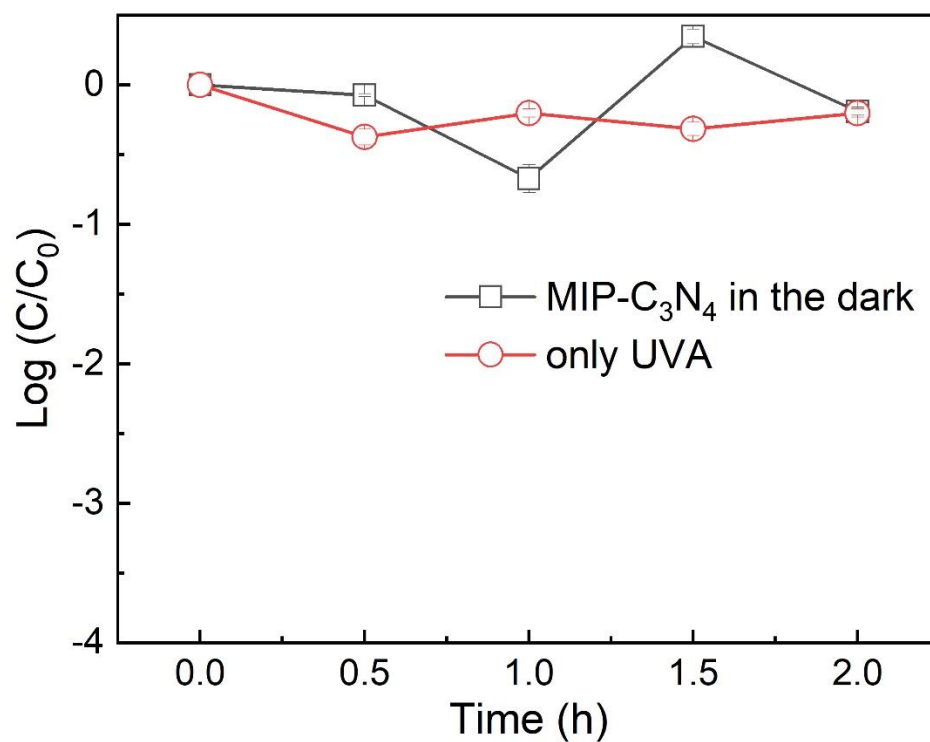


**Figure S8.** Lack of ARG removal in DI water by MIP-C<sub>3</sub>N<sub>4</sub> without UVA irradiation (after its ARG adsorption sites had been saturated), or by photolysis with UVA irradiation alone.

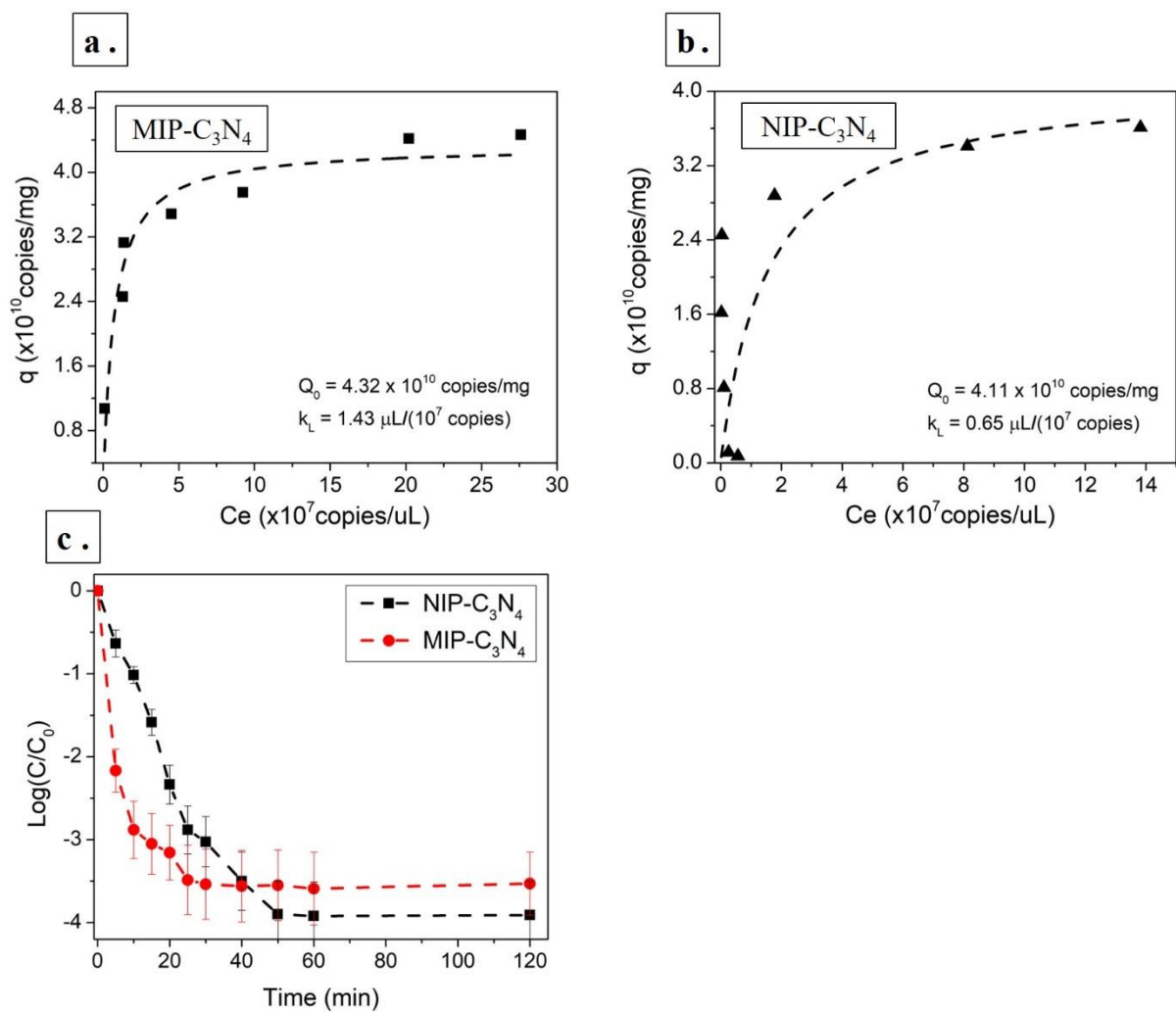
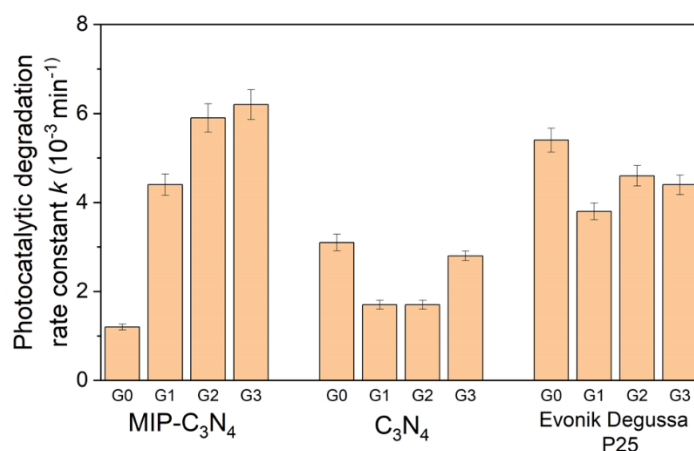


**Figure S9.** Adsorption isotherm (a, b) and kinetics (c) of *bla*<sub>NDM-1</sub> by MIP-C<sub>3</sub>N<sub>4</sub> or NIP-C<sub>3</sub>N<sub>4</sub> in DI water.

(a) Photocatalytic degradation



(b) Adsorption

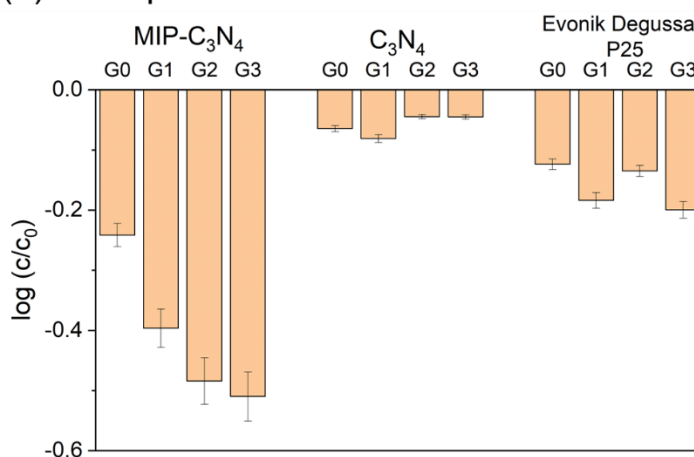


**Figure S10.** Photocatalytic degradation (a) and adsorption removal (b) of oligonucleotides with different guanine contents by MIP- $\text{C}_3\text{N}_4$ ,  $\text{C}_3\text{N}_4$ , and P25 in DI water. G0 (5'-CCCACCCACCCACCCAAA-3'), G1 (5'-GCCACCCACCCACCCAAA-3'), G2 (5'-CCCACCCACCGGCCCAA-3') and G3 (5'-CGCACCCACCGGCCCAA-3') contains zero, one, two and three guanines, respectively.

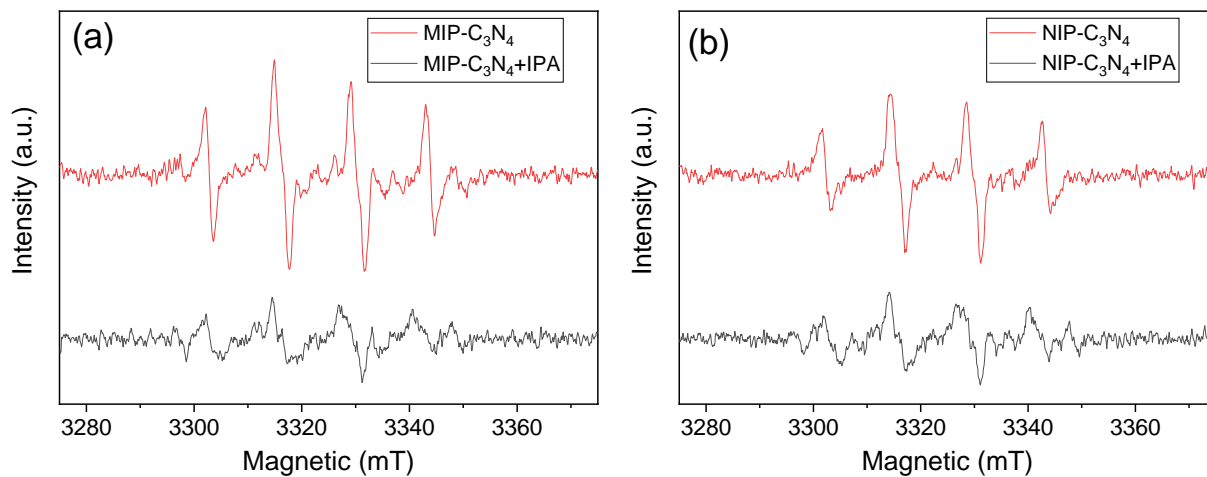


**Figure S11.** ESR spectra of MIP-C<sub>3</sub>N<sub>4</sub> (a) and NIP-C<sub>3</sub>N<sub>4</sub> (b) before and after spiking with •OH scavenger (IPA).

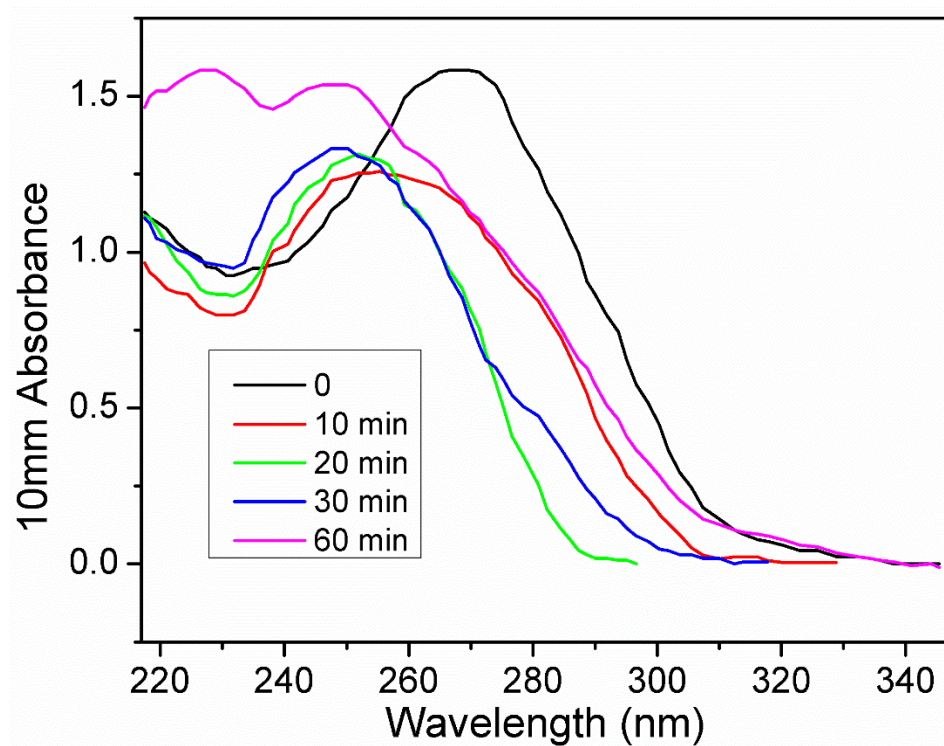


**Figure S12.** The UV-Vis spectrum of *bla*<sub>NDM-1</sub> sample treated by MIP-C<sub>3</sub>N<sub>4</sub> photocatalytic reaction at different times. The adsorption peak of *bla*<sub>NDM-1</sub> sample has a blue shift after treatment.

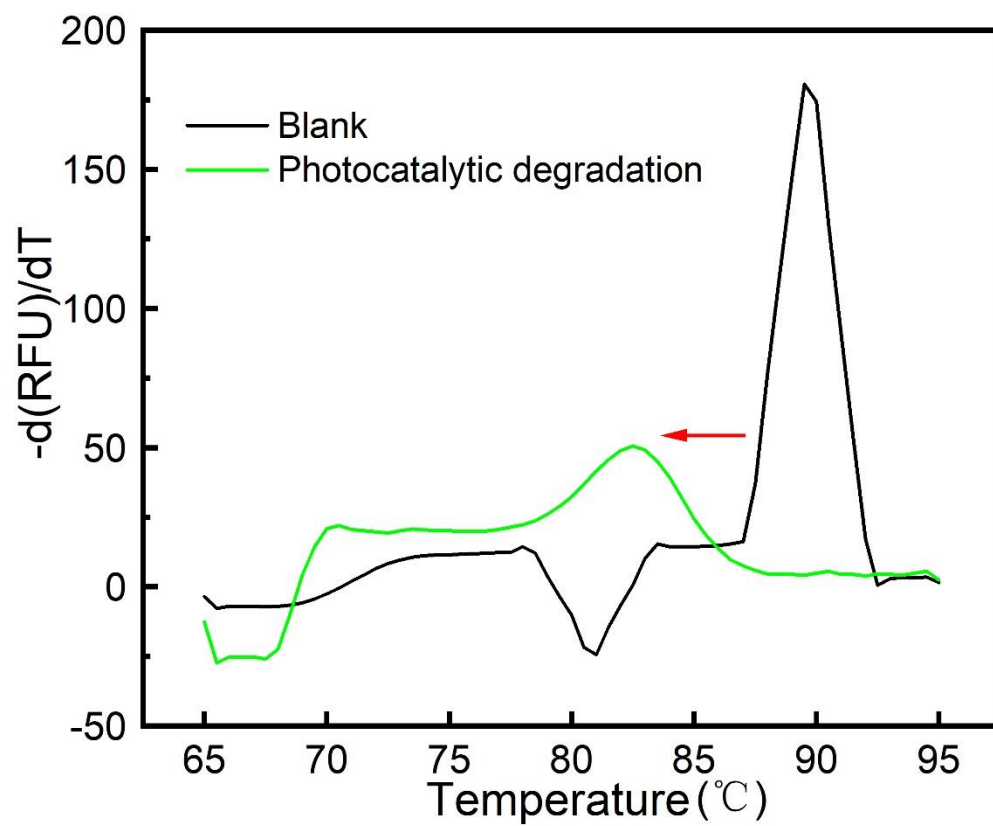


**Figure S13.** The melting curve of *bla*<sub>NDM-1</sub> sample treated by adsorption and photocatalytic reaction.



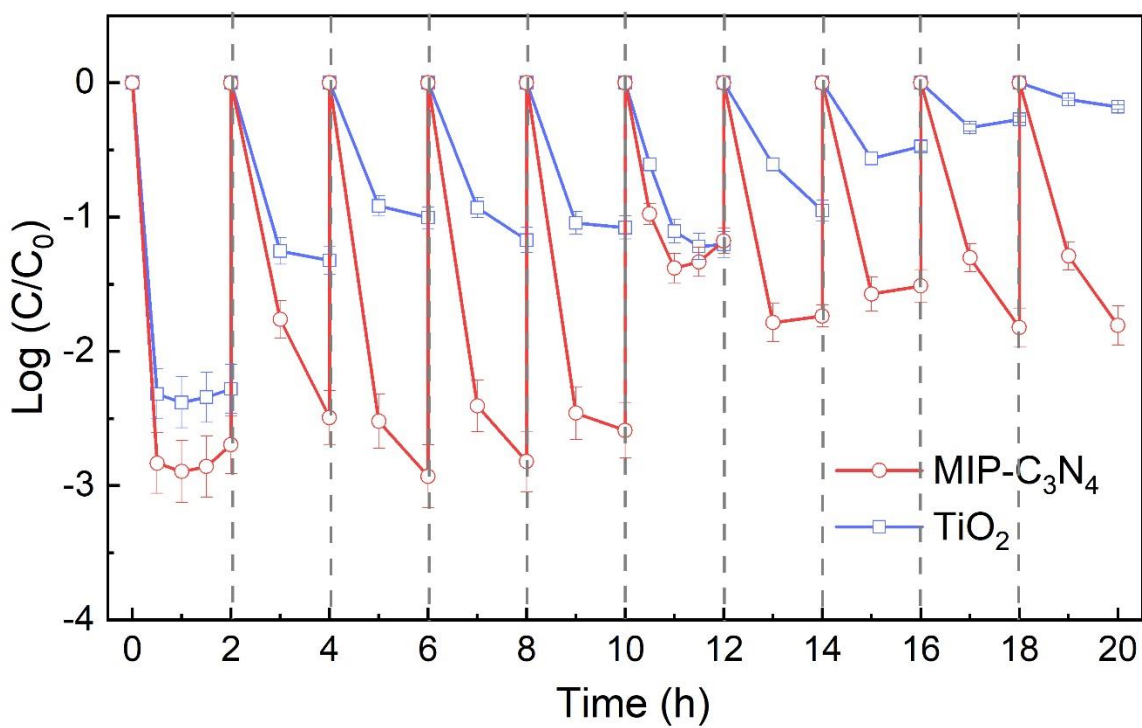


**Figure S14.** Reusability of MIP-C<sub>3</sub>N<sub>4</sub> and P25 TiO<sub>2</sub> in secondary effluent. Catalysts were tested for 10 cycles (2 hours for each cycle).

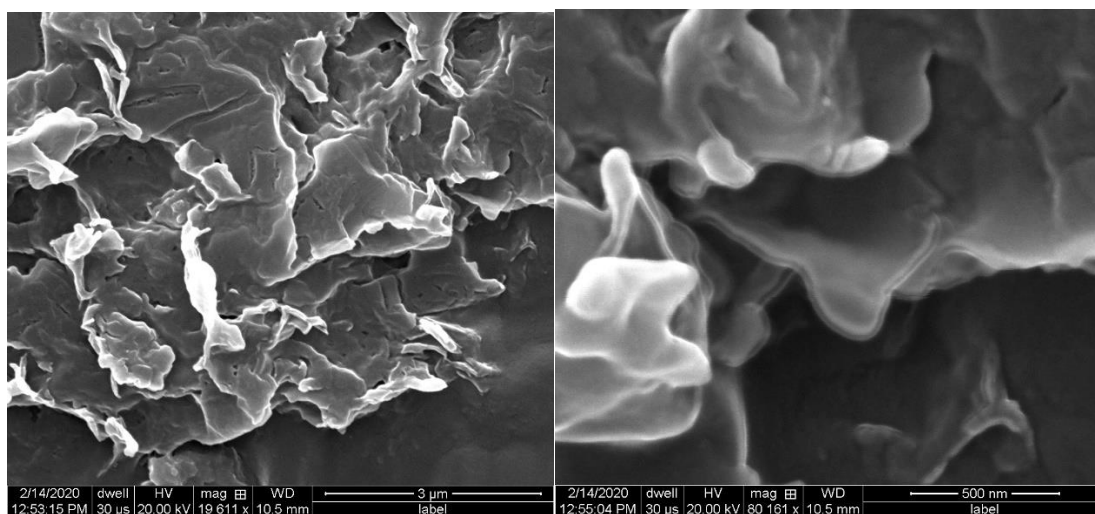


**Figure S15.** SEM images of MIP-C<sub>3</sub>N<sub>4</sub> after 10 cycles of reuse in secondary effluent.

**Table S1.** Water quality data of the secondary effluent from a wastewater treatment plant in Houston, TX (i.e., West University Place WWTP).

<sup>a</sup> TOC	pH	<sup>b</sup> DO	<sup>c</sup> TDS	Conductivity	<sup>d</sup> UV <sub>254</sub>
(mg/L)	(-)	(mg/L)	(mg/L)	(μS/cm)	(-)
16.1 ± 0.2	7.0 ± 0.01	6.9 ± 0.3	425 ± 17.5	770.7 ± 0.1	0.156 ± 0.001

<sup>a</sup> TOC: total organic carbon

<sup>b</sup> DO: dissolved oxygen

<sup>c</sup> TDS: total dissolved solid

<sup>d</sup> UV<sub>254</sub>: UV-absorbance at 254 nm

**Table S2.** Specific surface area of different catalysts.

Catalyst Name	Specific Surface Area (m <sup>2</sup> /g)
C <sub>3</sub> N <sub>4</sub>	85.4
MIP-C <sub>3</sub> N <sub>4</sub>	61.2
NIP-C <sub>3</sub> N <sub>4</sub>	60.5
TiO <sub>2</sub>	57.4

**Table S3.** Chemical bonds composition of MIP-C<sub>3</sub>N<sub>4</sub> pretreated with different oxidation time and their photoactivity in removing *bla*<sub>NDM-1</sub>.

Oxidation treatment duration (min)	Chemical bond composition (relative abundance, %)			Zeta potential (mV)	Photocatalytic degradation rate constant k (min <sup>-1</sup> )
	C-N	C-O-C	O=C-OH		
0	100 ± 0.1	NA	NA	0.42	NA
30	59.0 ± 0.3	22.4 ± 0.1	18.6 ± 0.2	-0.88	0.126 ± 0.023
60	47.2 ± 0.2	28.1 ± 0.2	24.7 ± 0.1	-1.08	0.084 ± 0.007
90	35.9 ± 0.1	33.9 ± 0.2	30.2 ± 0.3	-1.45	0.045 ± 0.004
120	31.3 ± 0.2	35.1 ± 0.3	33.6 ± 0.2	-1.58	0.045 ± 0.004

**Table S4.** First-order rate constant (k) of *bla*<sub>NDM-1</sub> removal by MIP-C<sub>3</sub>N<sub>4</sub> or NIP –C<sub>3</sub>N<sub>4</sub>, C<sub>3</sub>N<sub>4</sub> and TiO<sub>2</sub> (Evonik P25) in different water matrices.

Water matrix	Photocatalytic degradation rate constant k (min <sup>-1</sup> )			
	MIP-C <sub>3</sub> N <sub>4</sub>	NIP –C <sub>3</sub> N <sub>4</sub>	C <sub>3</sub> N <sub>4</sub>	P25
<b>DI water</b>	0.126 ± 0.023	0.123 ± 0.022	0.090 ± 0.020	0.116 ± 0.070
<b>Peptone (50 mg/L)</b>	0.114 ± 0.022	0.006 ± 0.012	—	—
<b>Sucrose (200 mg/L)</b>	0.117 ± 0.021	0.029 ± 0.01	—	—
<b>Humic Acid (10 mg/L)</b>	0.132 ± 0.022	0.006 ± 0.005	—	—
<b>Secondary effluent (TOC = 16.1 mg/L)</b>	0.111 ± 0.028	0.003 ± 0.003	0.003 ± 0.001	0.067 ± 0.009

**Table S5.** Total read count and average DNA length of *bla*<sub>NDM-1</sub> sample after treated by MIP-C<sub>3</sub>N<sub>4</sub> or NIP-C<sub>3</sub>N<sub>4</sub> in DI water.

Material	Reaction time (min)	Total read count	Average length (bp)
MIP-C <sub>3</sub> N <sub>4</sub>	10	7490	867.5
MIP-C <sub>3</sub> N <sub>4</sub>	60	1794	829.4
NIP-C <sub>3</sub> N <sub>4</sub>	120	5371	2675.3

## References

1. Teng, Z.; Yang, N.; Lv, H.; Wang, S.; Hu, M.; Wang, C.; Wang, D.; Wang, G. Edge-functionalized g-C<sub>3</sub>N<sub>4</sub> nanosheets as a highly efficient metal-free photocatalyst for safe drinking water. *Chem* **2019**, 5 (3): 664-680.